TOWARDS ISOLATED ROUGHNESS INDUCED BOUNDARY LAYER TRANSITION AT SUPERSONIC SPEEDS

Luis E. Mures González [1], Sam M Dakka[2]

[1](Department, Mechanical, Materials & Manufacturing Engineering/ University of Nottingham, United Kingdom)
[2](Department, Mechanical, Materials & Manufacturing Engineering / University of Nottingham, United Kingdom)

ABSTRACT : *The height of surface roughness elements affects the onset of laminar to turbulent transition in a boundary layer. CFD studies have been accomplished using RANS models at very low speeds, as a first step towards the understanding of this technology in supersonic/hypersonic flows. All simulations were performed on the commercial CFD program, ANSYS Fluent. Four flow cases have been investigated in this paper: natural transition of a 5.4 m/s flow over a flat plate, natural transition of a 9.8 m/s flow over a flat plate, implementation of a trip device in a 9.8 m/s flow and an attempt of capturing supersonic transition using a trip at Mach 3.5. Various turbulence models have been compared and the SST K-Omega gamma Transport model proved to capture the onset of transition with the best accuracy. The results concluded that a flow at 5.4 m/s naturally transitions 0.7 m downstream from the leading edge at $Re_x = 2.59 \times 10^5$. Additionally, a 9.8 m/s flow transitions 1.25 m downstream at $Re_x = 1.7 \times 10^6$. There is a difference of 0.55 m between these two values, highlighting the importance of roughness elements in high-speed flows. Both flows have been validated against experimental results from ERCOFTAC T3A and T3A- test cases. The implementation of a trip in the 9.8m/s flow moves the onset of transition further upstream. The critical height, in this case, is $k/_{\delta*} \approx 0.25$ and the effective height is $0.67 < k/_{\delta*} < 0.68$. Finally, an attempt to capture transition at Mach 3.5 using the same turbulence model did not achieve the desired results meaning other methods must be used in future work. With the limitations of physical testing capabilities for supersonic/hypersonic aerodynamics either due to the expense or unreliability of testing facilities, accurate CFD simulations of the effects of surface roughness are extremely important to contribute to ongoing research. There are many uses for this technology, ranging from commercial hypersonic flight to hypersonic missile systems.*

KEYWORDS - *Surface roughness element, boundary layer transition, ANSYS Fluent, CFD-Computational Fluid Dynamics.*

I.   INTRODUCTION

A roughness element or tripping device is a 3D object placed on the forebody of a craft to promote laminar to turbulent transition (LTT). It is known that geometrical parameters such as the shape, size and height of a roughness element directly influence the LTT in a boundary layer (BL) (Schneider, 2008) [1,2]. An accurate prediction of BL transition is extremely important as it is known to have a major impact on the design and performance of high-speed vehicles ('Pages - NATO Science & Technology Organization', n.d.) [3]. For high-speed flows, transition promotes an undesirable increase in skin friction and surface heating which, potentially could damage the structural integrity of a craft (Iyer & Mahesh, 2013) [4]. On the other hand, practical applications in which LTT is desirable exist.

A Scramjet is an engine that flies at supersonic speed and compresses the incoming air by the forward speed of the aircraft itself, as opposed to normal jet engines which require a rotary compressor section before combustion (NASA - How Scramjets Work, n.d.) [5]. Laminar air present at the entrance of a scramjet can be detrimental, as, under low Reynolds number conditions, the scramjet will be prone to large separation bubbles, which could lead to engine unstart (Hopkins, 2021) [6]. In scramjet applications, roughness elements are

employed on the forebody of high-speed vehicles to intentionally trip the BL from laminar to turbulent and improve engine operability. This technology has been proven to work on NASA's X-43A flight in 2004, which holds the record for the fastest flight for jet-powered aircraft, Mach 9.6 (NASA - the Record-Breaking Flights, n.d.) [7]. Some future applications for this technology may include, future hypersonic air-breathing commercial flights, Single Stage to Orbit (SSTO) vehicles or hypersonic missiles.

Past studies all agree that there has been great progress in the past two decades on the in-depth understanding of different transition methods. Although the physical mechanisms underlying the phenomenon of surface roughness induced transition are still far from being understood at this time (Gramespacher et al., 2021) [8] (Choudhari et al., 2010) [9] (Berry et al., 2001) [10] (Lee & Chen, 2018) [11]. In addition, flight data pertaining to this technology is limited and ground-based experimental data from wind tunnels are argued to not be reliable predictors of flight performance (Reed et al., 1997) [12] (Lee & Chen, 2018) [11] (Stetson, 1990) [13] (Chen et al., 1989) [14]. As there are uncertainties related to the experimental data of high-speed transition, completing accurate CFD simulations of transition is important to contribute to ongoing research. This project aims to use ANSYS Fluent to accumulate CFD results and complement existing experimentations to generate data on trip height, an important factor of influence of roughness induced LTT. This project will help the progress of innovative aerospace technologies in the space, commercial and defence sectors

II. BACKGROUND

2.1 Boundary Layer Theory

When an object is immersed and moving through a fluid where the effects of viscosity are significant, a thin layer of fluid surrounding the object is created. This layer of fluid is called the Boundary Layer (BL) or Fractional Layer. The concept of the BL was first identified by Ludwig Prandtl in 1904 (Tollmien et al., 1961) [15] and implies that flows at high Reynolds numbers can be divided into two unequally large separate flow regions: Outer and Inner flow. In the large outer flow region, the effect of viscosity is neglected, and the flow corresponds to the inviscid limiting solution. The second flow region is the BL near the wall. In this region, viscosity must be considered to satisfy the no-slip condition which, assumes that at a solid boundary the velocity of the fluid layer directly in contact with the boundary will be identical to the velocity of this surface. This creates a velocity gradient in the BL, where the velocity magnitude at the wall starts at zero and increases away from the wall until equal to the freestream velocity, (Boundary-Layer Theory, n.d.) [16].

Within the BL the flow can be in two forms: Laminar or Turbulent. Laminar or streamline flow can be defined as a flow in which the flow layers are in parallel with no disruption between the layers. Though, Turbulent flow is characterised by a "high irregular, random fluctuating motion" with large amounts of mixing perpendicular to the flow direction (Boundary-Layer Theory, n.d.) [16]. Correspondingly, turbulent flow experiences a steep velocity gradient at the wall and in turn large shear stresses and surface heating.

Flows can be transitional in nature, changing from laminar to turbulent. It is common that for many cases a flow analysis can be simplified, and the flow can be treated as either fully turbulent or fully laminar, as the transition may have a negligible effect on the performance of the system. Nevertheless, this is not true for certain applications.

For example, BL transition is known to have a substantial impact on the aerothermodynamic loading of hypersonic vehicles ('Pages - NATO Science & Technology Organization', n.d.) [3]. Also, the onset of transition along an aircraft's wing controls whether the flow will remain attached, become fully separated or form a separation bubble and reattach (Mankbadi, 1994) [17]. Finally, more specific for this report, transition before the inlet of a scramjet is desirable as it improves the engine's inlet operability (Hopkins, 2021) [6].

The Reynolds number was first introduced by George Stokes in 1851 (Stokes, 1851) [18] and was popularised by Osborne Reynolds in 1883 (Reynolds, 1883) [19]. The Reynolds number is the ratio of inertia forces to viscous forces and helps determine if a flow is either laminar or turbulent. When a Reynolds number is low, the viscous forces dominate, meaning the flow remains laminar. If the Reynolds number is large the inertial forces dominate, meaning the flow is turbulent.

Transitional flow takes place at a range of Reynolds numbers between laminar and turbulent. This range varies for different flow situations as every flow is different and has its own unique parameters. Therefore, there is no exact Reynolds number that guarantees a flow laminar or turbulent. A laminar flow may be maintained at much higher Reynolds numbers than normal if free stream turbulence levels and disturbances are kept to a minimum. Furthermore, turbulent flows can be seen at much lower Reynolds numbers if there is high free-stream turbulence, or if a tripping mechanism is used (Perrault, 2019) [20].

The strongest factors which influence the transition process are roughness, adverse pressure gradient and freestream turbulence (MIT Theses, n.d.) [21].

There are 3 main modes of transition:
- Natural transition
- Bypass transition
- Separated flow transition

Natural transition occurs in the BL at high Reynolds numbers and low freestream turbulence levels. The natural transition process starts with weak two-dimensional disturbances, known as Tollmien-Schlichting (T/S) waves, developing in the laminar flow. These waves start to destabilize and grow very slowly. The growth of these instabilities results in three-dimensional eddies and vortices in the BL. Next, the three-dimensional disturbances break down into spots of highly turbulent flow, which finally grow and expand into each other causing the BL to become fully turbulent.

Bypass Transition normally takes place due to some sort of external stimuli, such as high free-stream turbulence levels or surface roughness. In Bypass Transition the first three stages of transition which occur in natural transition are 'bypassed'. Turbulent spots are directly produced within the BL which expand and turn the BL fully turbulent.

If a laminar flow separates from the surface, either due to a tripping device or an adverse pressure gradient, transition may occur in the free shear-layer-like flow near the surface and reattach fully turbulent, creating a laminar separation bubble. The different stages of natural transition may or may not be present in this type of transition process.

Transition is a region; therefore, the definition of a transition point varies from paper to paper. In this paper, we consider the transition point as the point at which the flow becomes fully turbulent. The onset of transition is mentioned many times. This is referring to the position of this transition point.

2.2 Roughness Effects

Surface roughness elements alter the flow field over a surface by introducing velocity perturbations, increasing momentum deficit in the BL, and altering transition characteristics (Langel et al., 2017) [22]. As mentioned previously, a significantly important and frequently studied effect of roughness is a premature transition of the BL.

The geometrical characteristics of a roughness element such as height, shape and distribution are extremely important and must be taken into consideration, as they change how the flow interacts in the element.

The height 'k' of a tripping device plays an important role in the prediction of the onset of transition. Roughness elements shorter than the viscous sublayer normally don't influence the transition process. If 'k' is increased it will reach a value at which it will influence transition location, this height is called the 'critical height'. It is the minimum height of a trip device that has an impact on transition. If the height is further increased, the onset of transition will move further upstream towards the leading edge until it stagnates somewhere near the roughness. The minimum value of 'k' at which transition location stagnates just downstream of the roughness element is known as the 'effective height' (Schneider, 2008b) [2]. In scramjet applications, it is important to determine the value of this effective height. The ideal roughness element will trip the boundary layer rapidly without producing excessive amounts of drag. Hence, if the height exceeds the effective height the trip will produce unnecessary drag and surface heating.

As the BL doesn't have a constant thickness, the effects of roughness height cannot be generalised along the BL of a rough surface. As a result of this, it is common for studies to nondimensionalise the roughness

height with respect to the displacement thickness ($k/_{\delta*}$) or describe it using a roughness Reynolds number, Re_k, which can be defined as:

$$Re_k = \frac{\rho U_k k}{\mu} \qquad (1)$$

Where μ is the dynamic viscosity of the fluid, ρ is the density and U_k is the velocity in an undisturbed BL at height k. In this paper, we will nondimensionalize the roughness heights with respect to the displacement thickness.

2.3 Transition Prediction

The prediction of the onset of transition can prove challenging due to the different transition mechanisms and intricate sensitivities presented by different correlation criteria. Multiple methods have been proven to model the process of transition. These methods are either purely mathematical or correlation based on experimental observations. A common method of predicting transition is through Direct Numerical Simulation (DNS), which solves the Navier Stokes equations numerically without any turbulence model. At the present time, a drawback of DNS is that it is too computationally expensive for day-to-day simulations.

In this paper, the study of transition is accomplished using a correlation method using RANS models on Ansys fluent. There are multiple turbulence properties of interest for a flat plate such as wall skin friction, heat transfer, and profiles of velocity and temperature across the BL (Roy & Blottner, 2006) [23].

The skin friction coefficient has been used to visualise the transition region along the plate. The skin friction for laminar flows is smaller in magnitude compared to turbulent flows, therefore, a spike in skin friction can be seen during the transition.

III.   METHODOLOGIES

3.1 TEST CASE T3A FLAT PLATE TRANSITION

3.1.2 Problem Identification

A numerical simulation of a low-speed boundary layer transition over a flat plate is performed in this section. The computations were performed on the commercial CFD program, Ansys fluent and are based on an example case described in reference (Sanjay et al., 2019) [24], performed on the open-source tool, OpenFOAM®. Additionally, the results are compared to the "T3A" experiment on the ERCOFTAC (European Research Community on Flow, Turbulence and Combustion) database ('ERCOFTAC Classic Collection - Cases:Case020', n.d.) [25]. The T3A experiment performed by Coupland models a Flat-plate transitional 2D boundary layer flow with no pressure gradient or temperature variations through a closed-circuit wind tunnel described in Ryhming's test case specifications (Pironneau et al., 1992) [26]. In the experiment, free stream turbulence was measured using probe prongs which were placed on the test surface with the transverse proceeding three times the boundary layer thickness away from the test surface. The upstream free-stream velocity and turbulence intensity level for the T3A experiment are summarised in Table 1

Table 1 T3A Experiment Conditions

Case	Upstream Velocity (m/s)	Upstream turbulence intensity (%)	Turbulent Viscosity Ratio	Pressure gradient
T3A	5.4	3.0	12	0

3.1.3 Pre-Processing

The computational domain, plate geometry, boundary conditions and dimensions are shown schematically in Fig. 1 (Not to Scale) and Table 2. The flat plate is supplied with a no-slip boundary condition.
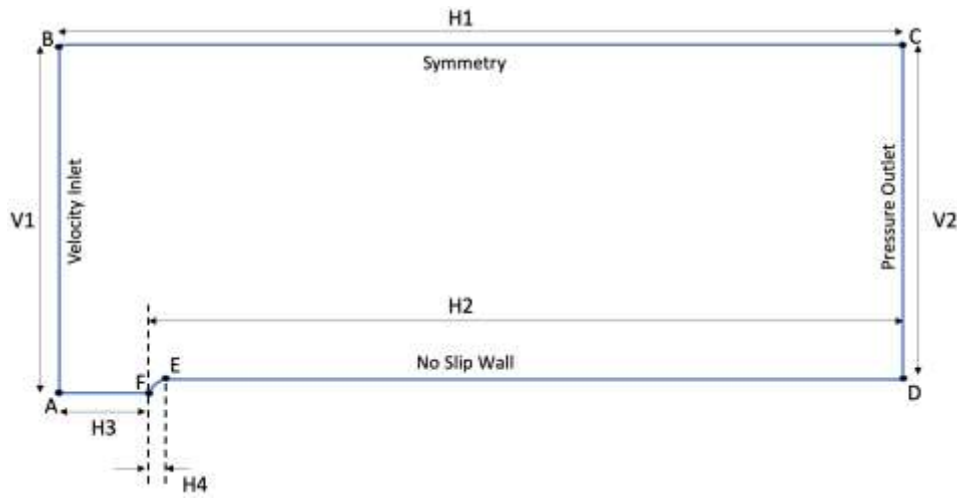

Figure 1 Schematic of Computational Domain

Table 2 *T3A Geometry Dimensions*

Dimensions (m)	
H1	3.000
H2	2..960
H3	0.040
H4	0.001
V1	1.000
V2	0.999

Boundary layers undergoing transition are much more sensitive to mesh resolution than fully laminar or turbulent flows. For transitional boundary layer flows Ansys provides a general recommendation for all transition models for mesh generation (Best Practice: RANS Turbulence Modeling in Ansys CFD, 2022) [27]:

- A streamwise grid step of $\Delta x = 1\delta$, Where δ is the Boundary layer thickness.
- $\Delta y_1^+ < 1$

A mesh sensitivity study is performed to ensure the simulation will acquire accurate results. The parameter of interest for this study is the Skin friction coefficient (Cf) along the flat plate therefore multiple meshes are refined until the "Cf" converged. The number of divisions along the X-axis was determined using the following equation for boundary layer thickness:

$$\delta_{99}(x) = 5\sqrt{\frac{vx}{U_\infty}} \qquad (2)$$

where v is the kinematic viscosity of air at sea level, x is the X position along the plate and U_∞ is the freestream velocity. A $\delta_{99}(x)$ of 5.25 mm was calculated for this flow speed, therefore the number of divisions needed to satisfy $\Delta y_1^+ < 1$, is approximately 600. Additionally, a bias factor of 200 along the Y-axis was set as the grid must be fine near the flat plate and leading-edge, to capture transition correctly. This value was kept constant throughout the mesh sensitivity study. Table 3 is a summary of all mesh configurations studied:

Table 3 *Mesh Sensitivity Study*

Mesh	Divisions along Y Axis	Divisions along X axis	Y+	Elements
1	100	600	1.75	6.19×10^4
2	150	600	1.40	9.27×10^4
3	200	600	1.18	1.24×10^5
4	300	600	0.79	1.85×10^5
5	350	600	0.65	2.16×10^5
6	400	600	0.57	2.47×10^5

A plot showing a comparison of all 6 mesh configurations can be seen in Fig. 2 below:
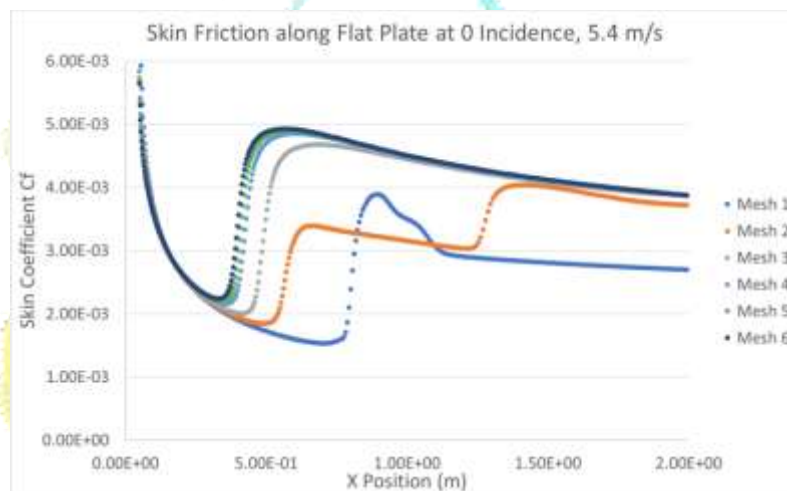

Figure 2 Skin Friction along Flat Plate at 0 incidence Plot

As the mesh is refined the values of the skin friction coefficient along the plate stagnate. Mesh 6 has a minimum orthogonal quality larger than 0.01. This mesh will be used for the remainder of the analysis.

The boundary conditions set are as follows:

- The inlet is set as a velocity inlet with a velocity magnitude of 5.4 m/s, turbulent intensity of 3% and a turbulent viscosity ratio of 12
- The outlet is set to a pressure outlet with a gauge pressure of 0 and turbulence properties identical to the inlet.
- The Fairfield is set as a symmetry boundary condition meaning the velocity of the flow is equal to the freestream value.
- The wall leading up to the leading edge of the plate is set as a stationary, no-slip wall.

3.1.4 Simulation Strategy

The simulation is solved using a pressure-based steady time solver. Alike reference (Sanjay et al., 2019) [24], the simulations are carried out using the transitional version of the SST k-Omega model. Although, Reference (Sanjay et al., 2019) [24] solves the Reynolds Averaged Navier Stokes Equations via the SIMPLE pressure-velocity coupling scheme. Test simulations were performed and showed that this strategy did not provide transition on ANSYS. Therefore, a COUPLED simulation was selected.

The simulation is split into two parts: first, the momentum, turbulent kinetic energy and specific dissipation rate are set to first-order upwind spatial discretization. Once the simulation was completed it is run again with second-order upwind spatial discretization with a residual absolute criterion of 0.0001.

3.1.5 Validation of Results

Post-processed results are presented in this section. The contour variation of turbulent kinetic energy near the transition region is shown in Fig. 3. The contour shows low kinetic energy over the initial portion of the flat plate, implying the boundary layer is laminar. The kinetic energy increases further down the plate meaning the boundary layer has transitioned from laminar to turbulent naturally.
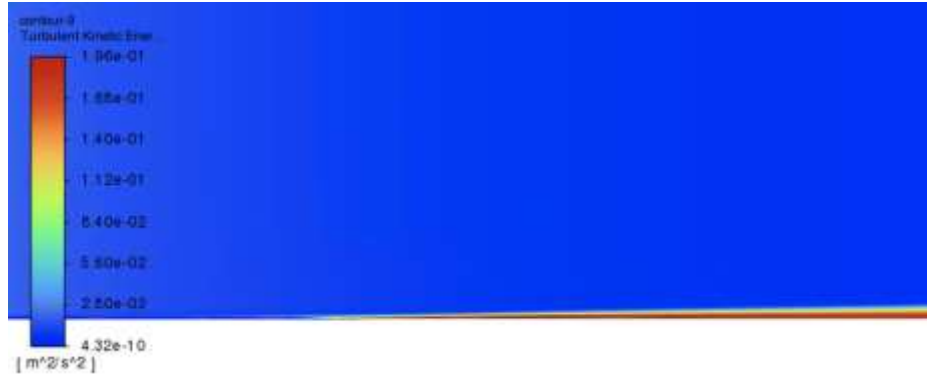

Figure 3 Zoomed T3A Contour of Turbulent Kinetic Energy

Fig. 4 shows a plot of the free-stream turbulent intensity against x, comparing the simulation results to the T3A experimental results. The simulated results match the experimental data and reveal how the intensity decays further downstream.
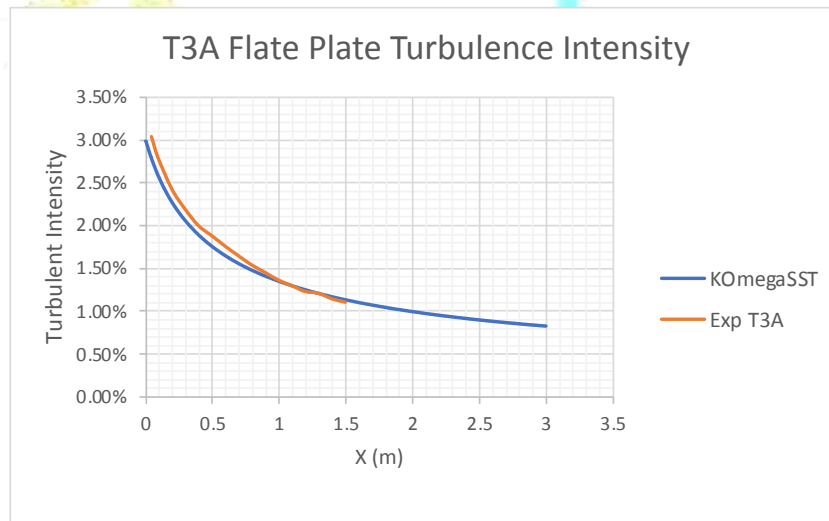

Figure 4 T3A Flat Plate Free Stream Turbulence Intensity

Finally, the coefficient of friction along the flat plate is plotted Fig. 5. The simulated results show a spike in the skin friction coefficient approximately 0.7m downstream from the leading edge. Experimental results indicate there is a transition region between 0.4m to 0.7m along the plate. The K-Omega SST Model shows similar results, but the onset of transition is 0.1 m earlier. Even though the computed flow becomes fully turbulent earlier compared to the experimental results, the actual transition region starts later, and the transition process occurs much quicker. The gradient of the K-Omega SST curve is larger.

The Reynolds number based on x, Re_x, at which the flow transitions has been calculated using the following equation:

$$Re_x = \frac{x \cdot U}{v} \qquad (3)$$

Where x is the position along the plate, U is the freestream velocity and v is the kinematic viscosity. The flow transitions at $Re_x = 2.59 \times 10^5$.
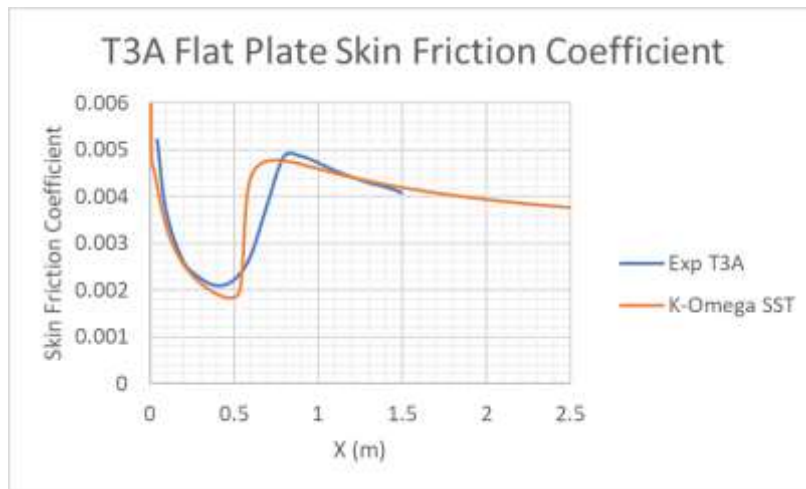
Figure 5 T3A Flat Plate Skin Friction Coefficient

In Fig 6 multiple turbulence models were compared to see which one captured the transition region more accurately. Even though again, the start of the transition process was computed later than experimental results, the K-Omega SST Gamma Transport model captured the onset of transition most accurately compared to the other models.
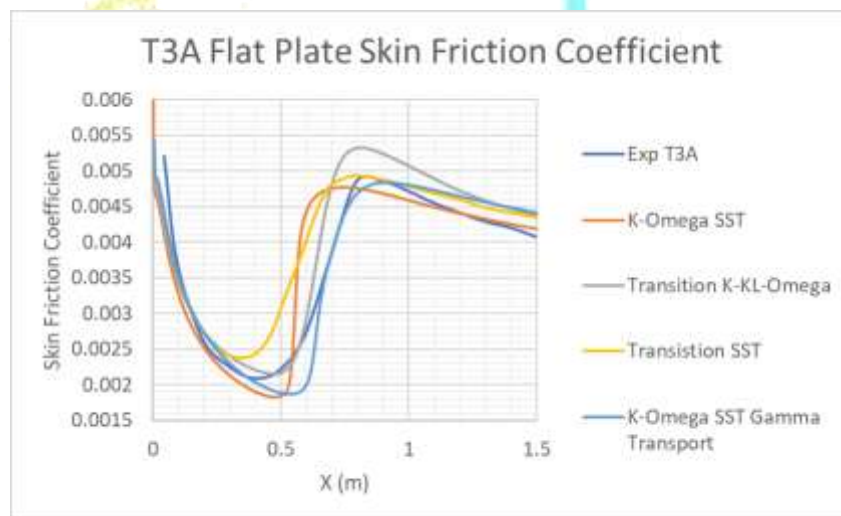

Figure 6 Comparison of Turbulence Models in the Transition region

3.2 Test Case T3A- Flat Plate Transition

3.2.1 Problem identification

Another simulation of higher speed, relative to the T3A case, is performed in this section. The reason behind this simulation is to view how the velocity magnitude affects the onset of transition. The results are compared and validated against the "T3A-" experiment on the ERCOFTAC database. In this experiment, the same wind tunnel was used as the T3A case. The upstream free-stream velocity and turbulence intensity level for the T3A- experiment are summarised in Table 4 below

Table 4 *T3A- Experiment Conditions*

Test Case	Upstream Velocity (m/s)	Upstream Turbulence Intensity	Turbulent Viscosity Ratio	Pressure gradient
T3A-	19.8	0.874	8.72	0

3.2.2 Pre-Processing

The computational domain and geometry dimensions are identical to the first T3A simulation done in the previous section.

Y+ can be described by the equation below:

$$Y^+ = \frac{U_\tau y_p \rho}{\mu} \qquad (4)$$

Where U_τ is the friction velocity, y_p is the distance of the first cell centroid from the nearest wall, ρ is the density of air at sea level and μ is the kinematic viscosity. As friction velocity is dependent on the inlet velocity, the increase in velocity in the T3A- case implies that the distance of the first cell centroid from the nearest wall must decrease to maintain $Y^+ < 1$. For this reason, a new mesh sensitivity study is performed.

As is $\delta_{99}(x)$ is now 7.44 mm the number of divisions required along the x-axis to satisfy the $\Delta x = 1\delta$ condition mentioned previously, has decreased to 398 divisions. Nonetheless, the x-axis division has remained at 600, since if it is decreased the difference in element sizes in the different sections of the mesh leads to non-convergence. Table 5 below is a summary of all mesh configurations studied and Fig. 7 shows a plot showing a comparison of all 5 mesh configurations.

Table 5 Case T3A- Mesh configurations

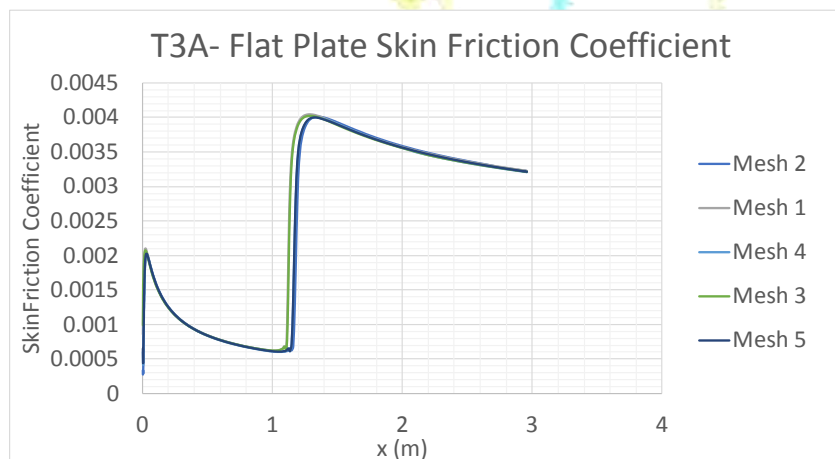| Mesh	Divisions along Y Axis	Divisions along X axis	Y+	Elements
1	400	600	2	2.47×10^5
2	500	600	1.7	3.24×10^5
3	700	600	1.2	4.45×10^5
4	800	600	1	5.18×10^5
5	850	600	0.9	5.48×10^5

Figure 7 T3A- Mesh Sensitivity Study

Mesh 5 was selected as the $Y^+ < 1$ and the solution stagnated.
The boundary conditions are identical to the T3A case except for the following changes:
- The inlet is set as a velocity inlet with a velocity magnitude of 19.8 m/s, turbulent intensity of 0.874% and a turbulent viscosity ratio of 8.72.
- The outlet is set to a pressure outlet gauge pressure of 0 and turbulence properties identical to the inlet.

3.2.3 Simulation Strategy

Again, the simulation was solved using a pressure-based steady time solver. The solution was solved using the coupled pressure-velocity coupling scheme with a momentum-based flux type. Additionally, the turbulence model used to predict the onset of transition is SST K-omega Gamma Transport and, SST K-Omega gamma algebraic was used to compare the free stream turbulence intensity which is discussed in the next section.

IV. VALIDATION

The post-processed results are shown in this section. Fig. 8 the transition region can be clearly seen with an increase in turbulent kinetic energy.
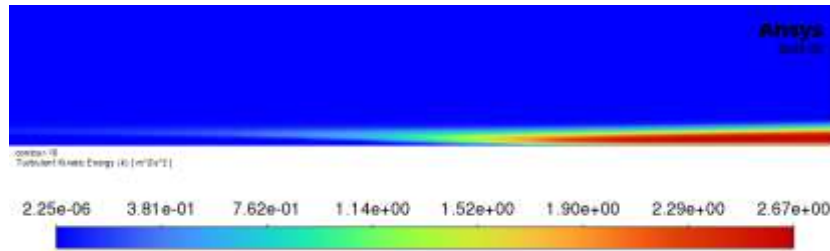
Figure 8 TKE contour of Onset of Transition

Fig. 9 below shows a plot of the free-stream turbulence intensity calculated in the same way as in test case T3A. The results show that the computational solution matches the experimental data.

Figure 9 *T3A- Flat Plate Turbulence Intensity*

As mentioned in the previous section, SST K-Omega Gamma Transport was used to capture the transition region as SST K-Omega could not. Fig. 10 shows how the model predicts transition earlier than what has been recorded in the experiment.

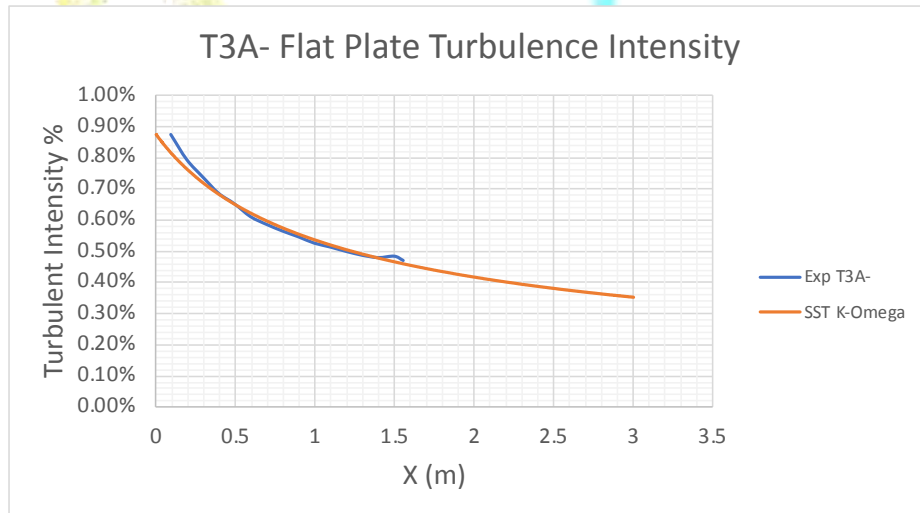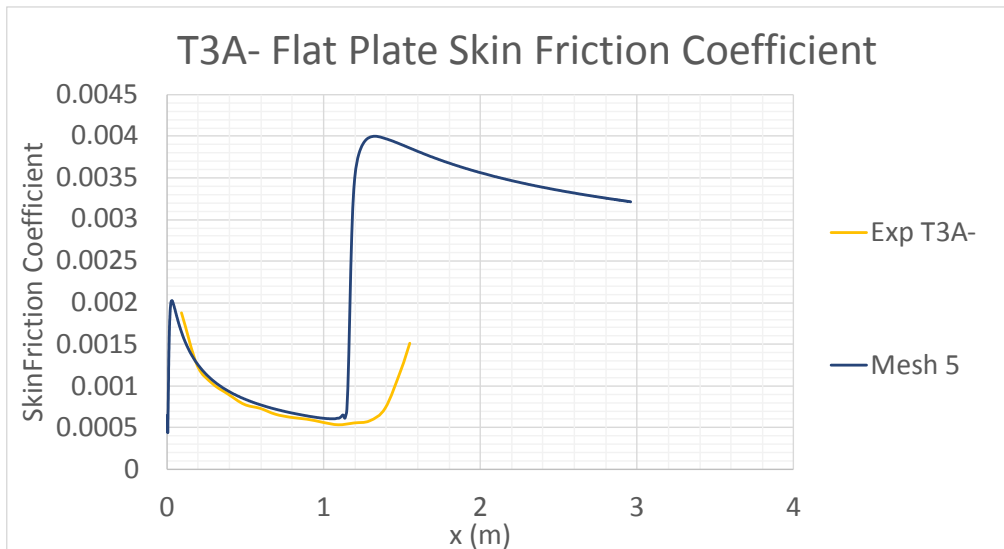**Figure 10** T3A- Flat Plate Skin Friction Coefficient

It is clear after running both cases, T3A and T3A-, that as the freestream velocity increases the onset of transition moves further down the plate. The simulation has predicted the onset of transition to be approximately 1.25 m downstream of the leading edge of the plate. This is 0.55 m further downstream than the T3A case. Additionally, the Reynolds number at which transition is seen is $Re_x = 1.7 \times 10^6$. This is the reason why tripping devices are needed in supersonic (1.2<M<5) and hypersonic (M>5) flows before a scramjet inlet. The flow is travelling at such high speeds that the flow can't naturally transition before it has reached the inlet.

V. IMPLEMENTATION OF ISOLATED 2D ROUGHNESS ELEMENT TO T3A- LOW-SPEED FLOW

5.1 Problem Identification

In this section, a 2D isolated roughness element is implemented near the leading edge of the plate. The goal of this analysis is to see how the height of this device affects the onset of transition. The 'critical' and 'effective' heights mentioned are determined for case T3A- 's flow conditions (19.8 m/s).

5.2 Pre-processing

Here the boundary conditions and mesh properties are identical to the previous T3A- case. Although the geometry has been adapted to implement the device as seen in Fig. 11
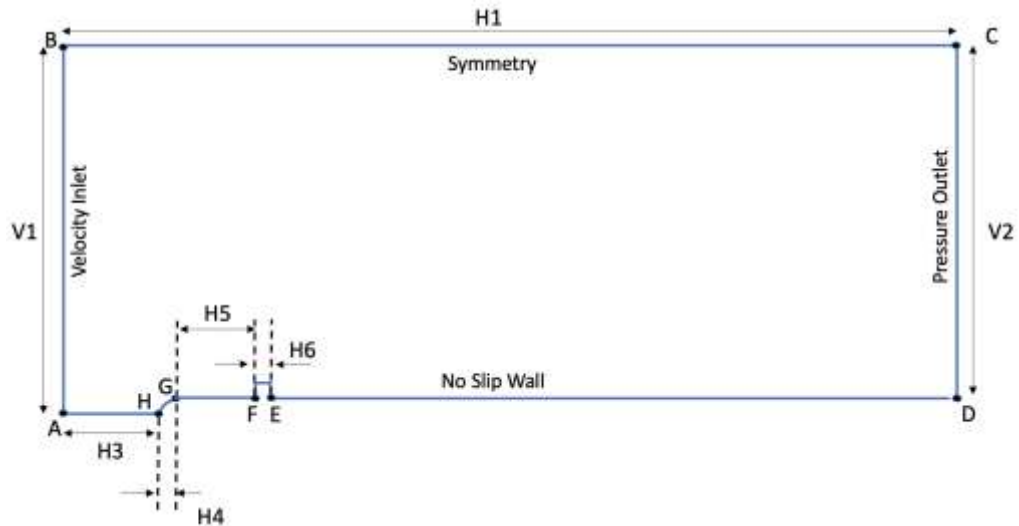
Figure 11 Low Speed Trip Geometry

The tripping device is diamond in shape, based on supersonic/hypersonic devices studied in references (Choudhari et al., 2010) [9] (Estruch-Samper et al., 2017) [28]. Additionally, the trip is placed 4 cm downstream of the leading edge as in done in reference (Choudhari et al., 2010) [9]. A schematic of the diamond trip used in reference (Choudhari et al., 2010) [9] can be seen in Fig. 12.
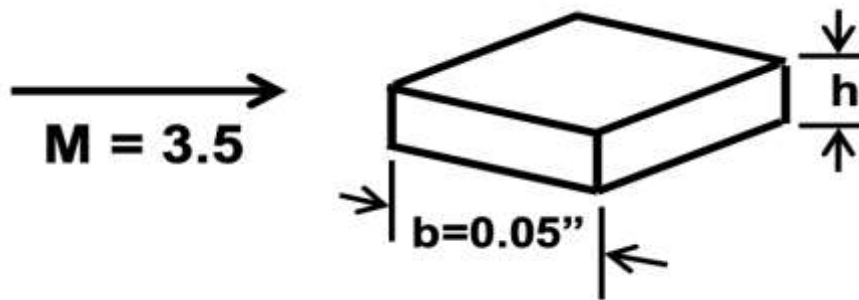
Figure 12 *Schematic of diamond trip*

Key dimensions are listed below in Table 6 (Identical dimensions to T3A and T3A- case have been left out):

Table 6 Trip Device Implementation Case Key Dimensions

Dimensions (m)	
H1	3
H5	0.0413
H6	0.0018

5.3 Simulation Strategy

The simulation strategy is identical to the T3A and T3A- cases.

VI.   RESULTS & DISCUSSION

As mentioned previously the height of the trip device, 'k', can be non-dimensionalised with respect to the boundary layer height, $k/_{\delta*}$. The undisturbed boundary layer height at the location of the trip can be calculated using equation 2, Multiple trip heights are used to find effective and critical heights. A few are listed in Table 7 below:

Table 7 *Trip Heights*

$k/_{\delta*}$	k
0.25	0.218
0.65	0.567
0.66	0.575
0.662	0.577
68%	0.593

Fig. 13 shows a plot of the skin friction coefficients for the various trip height configurations along the plate.

Figure 13 Skin Friction Coefficient Comparison for Various Trip Heights

Additionally, Figure 14 gives a more comprehensible view of how the onset of transition is moving forward towards the leading edge of the plate. The figure shows a comparison of the turbulent intensity contours given by various trip heights shown as a percentage of the undisturbed boundary layer height at the position of the trip. The white lines represent an approximation of the onset of transition.

Figure 14 Comparison of Contours for Various Trip Heights

As you can see in Figure 15, as $k/_{\delta*}$ surpasses 0.25 the onset of transition gradually starts to move upstream. It seems that at the beginning a large change in $k/_{\delta*}$ from 0.25 to 0.66 moves the transition point approximately 0.3m upstream. Once $k/_{\delta*}$ is larger than 0.66 the onset of transition moves extremely quickly upstream. Between $k/_{\delta*} = 0.66$ and 0.67 the transition point moves approximately 0.6 m upstream. This can be observed more clearly.

After analysing these results, the critical and effective trip heights were determined. The critical height, in this case, is $k/\delta_* \approx 0.25$ and the effective height is $0.67 < k/\delta_* < 0.68$.
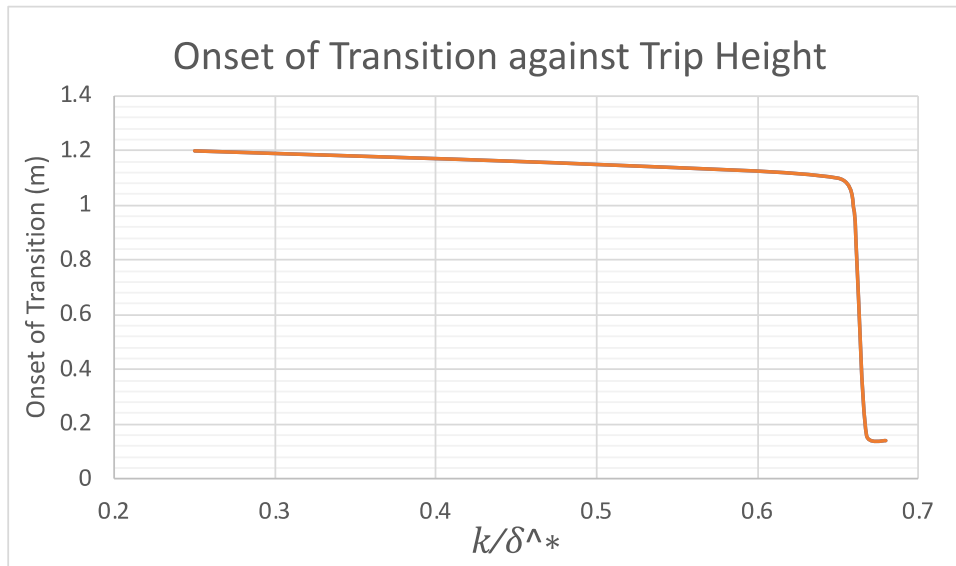

Figure 15 Onset of Transition against Trip Height

6.1 SUPERSONIC FLAT PLATE TRANSITION

A supersonic flow no longer can be assumed to be incompressible. Compressibility makes the stability and transition problems more complex and realistic. In this section, an attempt to model a Mach 3.5 flow over the previous flat plate and trip geometry is discussed. Pressure inlet and outlets must be used for a supersonic compressible flow. The static pressure and temperature were determined from the ISA table at sea level. These values were used in the isentropic flow relations shown in equations 5 and 6 to calculate the total pressure and temperature.

$$\frac{p_t}{p} = \left(1 + \frac{\gamma-1}{2}M^2\right)^{\frac{\gamma}{\gamma-1}} \tag{5}$$

$$\frac{T_t}{T} = 1 + \frac{\gamma-1}{2}M^2 \tag{6}$$

Where, γ is the specific heat ratio, M is the Mach number, p is the static pressure, p_t is the stagnation pressure, T is the temperature and T_t is stagnation temperature.

Table 8 provides a summary of the selected parameters and operating conditions used within the simulation.

Table 8 Supersonic Simulation Parameters

Parameter	Input
CFD Solver	Density-Based
Energy Equation	On
Density	Ideal gas
Viscosity	Sutherland
Turbulence Model	SST K-Omega Gamma Transport
Pressure Inlet	$p_t = 7728290.6\ pa$ $p = 101325pa$ $T_t = 994.1k$
Pressure Outlet	$p = 0pa$ $T_t = 994.1k$

According to paper (Choudhari et al., 2010) [9] a trip height of approximately 0.3048 mm in a Mach 3.5 flow should see a transition point 0.2 m downstream. The simulations were performed and did not give the desired results as mentioned in paper (Choudhari et al., 2010) [9].

VII. CONCLUSION

In conclusion, the computational studies done on ANSYS fluent following flow conditions provided by ERCOFTAC for both test cases T3A and T3A- agree with the experimental results. It has been concluded that the turbulence model SST k-Omega gamma transport captures the onset of transition best in all cases. For the 5.4 m/s T3A case the analysis proves that the onset of natural transition can be seen 0.7 m downstream from the leading edge at $Re_x = 2.59 \times 10^5$. Furthermore, SST K-Omega gamma transport predicts the onset of transition for the 19.8 m/s T3A- case approximately 1.25 m downstream at $Re_x = 1.7 \times 10^6$. This is 0.55 m further downstream than the first T3A, proving the importance of tripping devices for high-speed flows.

Moreover, a tripping device has been implemented on the flat plate 4 cm downstream from the leading edge at flow conditions matching the T3A- case. At a specific height, this device causes the onset of LTT transition to move upstream reducing the Reynolds number at which the flow transitions. It was determined that the non dimensionalized critical height for this flow is approximately 0.25. Additionally, the non dimensionalized effective height can be assumed to be between 0.67 and 0.68.

Finally, a Mach 3.5 supersonic flow has been modelled over a flat plate seen and the tripping device configuration is used in section 3.3. It was concluded that the transition model used for prior simulations was not capable of capturing the transition region. The next step in this research is to use other computational methods to capture transition in both supersonic and hypersonic flows.

In future work, the plan is to develop on the current research achieved and move on to capturing three-dimensional isolated roughness induced supersonic and hypersonic transition regions. Throughout this paper, the authors used a correlation method on Ansys Fluent to capture transition at low-speed conditions. It is known that conventional (RANS) averaging procedures are not the best solution for transitional flows where linear and nonlinear effects are relevant. Furthermore, transition occurs through different mechanisms which are difficult to capture all through one model (Menter, Langtry, & Völker, 2006) [29].

For this reason, in future studies, other methods based on either stability theory, intermittency factors, amplitude streamwise fluctuations, etc could be used to obtain much better results.

This can be achieved with the use of recent modified existing RANS CFD codes with the capability of onset prediction such as "LCTM" (Menter et al., 2006) [30], "Walters and Leylek model" (Walters & Leylek, 2004) [31] or "Suzen and Huang model" (Suzen & Huang, 2000) [32] could be used to obtain much better results.

Finally, in the future when direct numerical simulation (DNS) and Large Eddies Simulation (LES) become less computationally expensive and more suitable for day-to-day simulations, they can be used to study instabilities in the transition region with much more detail.

REFERENCES

[1] Schneider, S. P. (2008a, March). Effects of Roughness on Hypersonic Boundary-Layer Transition. *Journal of Spacecraft and Rockets*, *45*(2), 193–209. https://doi.org/10.2514/1.29713

[2] Schneider, S. P. (2008b, March). Effects of Roughness on Hypersonic Boundary-Layer Transition. *Journal of Spacecraft and Rockets*, *45*(2), 193–209. https://doi.org/10.2514/1.29713

[3] Pages - NATO Science & Technology Organization. (n.d.). *NORTH ATLANTIC TREATY ORGANIZATION, SCIENCE AND TECHNOLOGY ORGANIZATION, AC/323(AVT-240) TP/902, Hypersonic Boundary-Layer Transition Prediction*. Retrieved 8 October 2022, from https://www.sto.nato.int/

[4] Iyer, P. S., & Mahesh, K. (2013, July 24). High-speed boundary-layer transition induced by a discrete roughness element. *Journal of Fluid Mechanics*, *729*, 524–562. https://doi.org/10.1017/jfm.2013.311

[5] *NASA - How Scramjets Work*. (n.d.). Retrieved 8 October 2022, from https://www.nasa.gov/centers/langley/news/factsheets/X43A_2006_5.html

[6] Hopkins, K. J. (2021, July 14). *Measurements and analysis of hypersonic tripped boundary layer turbulence*. SpringerLink. Retrieved 8 October 2022, from https://link.springer.com/article/10.1007/s00348-021-03254-z?error=cookies_not_supported&code=07d34bf4-217f-4966-a680-73f22034b622

[7] *NASA - The Record-Breaking Flights*. (n.d.). Retrieved 8 October 2022, from https://www.nasa.gov/centers/langley/news/factsheets/X43A_2006_3.html

[8] Gramespacher, C., Stripf, M., & Bauer, H. J. (2021, November 2). The Influence of Deterministic Surface Roughness and

Freestream Turbulence on Transitional Boundary Layers: Heat Transfer Distributions and a New Transition Onset Correlation. *Journal of Turbomachinery*, *144*(4). https://doi.org/10.1115/1.4052458

[9]   .Choudhari, M., Li, F., Chang, C. L., Edwards, J., Kegerise, M., & King, R. (2010, January 4). LLaminar-Turbulent Transition behind Discrete Roughness Elements in a High-Speed Boundary Layer. *48th AIAA Aerospace Sciences Meeting Including the New Horizons Forum and Aerospace Exposition*. https://doi.org/10.2514/6.2010-1575

[10]   Berry, S. A., Auslender, A. H., Dilley, A. D., & Calleja, J. F. (2001, November). Hypersonic Boundary-Layer Trip Development for Hyper-X. *Journal of Spacecraft and Rockets*, *38*(6), 853–864. https://doi.org/10.2514/2.3775

[11]   Lee, C., & Chen, S. (2018, May 7). Recent progress in the study of transition in the hypersonic boundary layer. *National Science Review*, *6*(1), 155–170. https://doi.org/10.1093/nsr/nwy052

[12]   Reed, H., Kimmel, R., Schneider, S., Arnal, D., Reed, H., Kimmel, R., Schneider, S., & Arnal, D. (1997, June 29). Drag prediction and transition in hypersonic flow. *28th Fluid Dynamics Conference*. https://doi.org/10.2514/6.1997-1818

[13]   Stetson, K. F. (1990). Hypersonic Transition Testing in Wind Tunnels. *Advances in Soil Science*, 91–100. https://doi.org/10.1007/978-1-4612-3430-2_13

[14]   Chen, F. J., Malik, M. R., & Beckwith, I. E. (1989, June). Boundary-layer transition on a cone and flat plate at Mach 3.5. *AIAA Journal*, *27*(6), 687–693. https://doi.org/10.2514/3.10166

[15]   Tollmien, W., Schlichting, H., Görtler, H., & Riegels, F. W. (1961). Über Flüssigkeitsbewegung bei sehr kleiner Reibung. *Ludwig Prandtl Gesammelte Abhandlungen*, 575–584. https://doi.org/10.1007/978-3-662-11836-8_43

[16]   *Boundary-Layer Theory*. (n.d.). SpringerLink. Retrieved 8 October 2022, from https://link.springer.com/book/10.1007/978-3-662-52919-5?error=cookies_not_supported&code=12097c87-005c-4cf7-83b6-23c4d8920068

[17]   Mankbadi, R. R. (1994). Later Stages of Boundary-Layer Transition. *Transition, Turbulence, and Noise*, 51–82. https://doi.org/10.1007/978-1-4615-2744-2_3

[18]   .Stokes, G. G. (1850). On the effect of internal friction of fluids on the motion of pendulums. *Trans. Camb. phi1. S0c*, *9*(8), 106.

[19]   Reynolds, O. (1883). XXIX. An experimental investigation of the circumstances which determine whether the motion of water shall be direct or sinuous, and of the law of resistance in parallel channels. *Philosophical Transactions of the Royal society of London*, (174), 935-982.

[20]   Perrault, A. J. (2019, May 24). *Computational Simulations of Compressible Transitional Flows in a Turbine Vane Cascade*. Retrieved 8 October 2022, from https://library.ndsu.edu/ir/handle/10365/29783

[21]   *MIT Theses*. (n.d.). Retrieved 8 October 2022, from http://dspace.mit.edu/handle/1721.1/7582

[22]   Langel, C. M., Chow, R., & Maniaci, D. (2017, October 1). A Transport Equation Approach to Modeling the Influence of Surface Roughness on Boundary Layer Transition. *Technical Report*. https://doi.org/10.2172/1596203

[23]   Roy, C. J., & Blottner, F. G. (2006, October). Review and assessment of turbulence models for hypersonic flows. *Progress in Aerospace Sciences*, *42*(7–8), 469–530. https://doi.org/10.1016/j.paerosci.2006.12.002

[24]   Sanjay, S., Sundararaj, S., & Thiagarajan, K. B. (2019). Numerical simulation of flat plate boundary layer transition using OpenFOAM®. *AIP Conference Proceedings*. https://doi.org/10.1063/1.5112319

[25]   ERCOFTAC Classic Collection - cases:case020. (n.d.). *Flat Plate Transitional Boundary Layers*. Retrieved 8 October 2022, from http://cfd.mace.manchester.ac.uk/ercoftac/doku.php?id=cases:case020

[26]   Pironneau, O., Rodi, W., Ryhming, I. L., Savill, A. M., & Truong, T., V. (1992, July 31). *Numerical Simulation of Unsteady Flows and Transition to Turbulence* (1st ed.). Cambridge University Press.

[27]   *Best Practice: RANS Turbulence Modeling in Ansys CFD*. (2022, July 29). Ansys. Retrieved 8 October 2022, from https://www.ansys.com/en-gb/resource-center/technical-paper/best-practice-rans-turbulence-modeling-in-ansys-cfd

[28]   Estruch-Samper, D., Hillier, R., Vanstone, L., & Ganapathisubramani, B. (2017, April 4). Effect of isolated roughness element height on high-speed laminar–turbulent transition. *Journal of Fluid Mechanics*, *818*. https://doi.org/10.1017/jfm.2017.160

[29]   Menter, F. R., Langtry, R., & Völker, S. (2006, August 18). Transition Modelling for General Purpose CFD Codes. *Flow, Turbulence and Combustion*, *77*(1–4), 277–303. https://doi.org/10.1007/s10494-006-9047-1

[30]   Menter, F. R., Langtry, R. B., Likki, S. R., Suzen, Y. B., Huang, P. G., & Völker, S. (2006). A Correlation-Based Transition Model Using Local Variables—Part I: Model Formulation. *Journal of Turbomachinery*, *128*(3), 413. https://doi.org/10.1115/1.2184352

[31]   Walters, D. K., & Leylek, J. H. (2004, January 1). A New Model for Boundary Layer Transition Using a Single-Point RANS Approach. *Journal of Turbomachinery*, *126*(1), 193–202. https://doi.org/10.1115/1.1622709

[32]   Suzen, Y., & Huang, P. (2000, January 10). An intermittency transport equation for modeling flow transition. *38th Aerospace Sciences Meeting and Exhibit*. https://doi.org/10.2514/6.2000-287